Forest Ecology and Management 390 (2017) 89–103

Contents lists available at ScienceDirect

Forest Ecology and Management

journal homepage: www.elsevier.com/locate/foreco

Local soil type variability controls the water budget and stand productivity in a beech forest

Gil Kirchen [a], Christophe Calvaruso [a,b], André Granier [c], Paul-Olivier Redon [d], Grégory Van der Heijden [a], Nathalie Bréda [c], Marie-Pierre Turpault [a,*]

[a] UR "Biogeochemistry of Forest Ecosystems", UR1138, Centre INRA de Nancy, 54280 Champenoux, France
[b] EcoSustain, Environmental Engineering Office, Research and Development, 57330 Kanfen, France
[c] UMR "Forest Ecology and Ecophysiology", UMR1137, INRA – Université de Lorraine, 54280 Champenoux, France
[d] Andra, R&D Division, Centre de Meuse/Haute-Marne, 55290 Bure, France

ARTICLE INFO

Article history:
Received 23 September 2016
Accepted 21 December 2016

Keywords:
Water balance
Beech forest ecosystem
Soil type
Water holding capacity
Soil water drainage
Drought
Stand growth
Water use efficiency

ABSTRACT

Climate change and particularly increasing frequency of drought events during the vegetation period may threaten tree vitality and forest biomass productivity in many temperate regions in the future. In that context, the identification of critical environmental factors and a better understanding of their impact on forests are decisive. The water balance is recognized as one of the most important soil factors for stand productivity in temperate forests. Hence, the consequences of short or long term climate change might vary considerably spatially in function of soil type within a given forest. Our study objective was to assess the impact of contrasting soil types on the water balance and stand growth of a beech (*Fagus sylvatica*) forest ecosystem of similar age and management during four climatically contrasting years. The experimental forest site of Montiers presents different soils with contrasting physicochemical properties (Dystric Cambisol, Eutric Cambisol and Rendzic Leptosol) monitored to quantify water fluxes and stand biomass increment. Using data collected over the period 2012–2015, including a particularly dry year (−24% precipitations in 2015), we also quantified the impact of water shortage on stand productivity at the annual scale as a function of soil type. We evidenced important differences in soil water holding capacities (SWHC) along the studied soil sequence, ranging between 57 mm for the Rendzic Leptosol downhill over limestone and 205 mm for the Dystric Cambisol uphill over detrital sediments. The results show that the canopy intercepted the same amount of incident rainfall in the three plots and that there were no significant differences in annual soil moisture dynamics among the studied soils. We evidenced different rooting patterns depending on soil type. Under a same climate and with stand, site exposition and solar radiation equivalency, trees transpiration was the evident primary driver of the stand potential to produce aboveground biomass. Soil water holding capacity, annual trees transpiration and aboveground biomass production increased in that order: Rendzic Leptosol < Eutric Cambisol < Dystric Cambisol. During the drier year 2015, the decrease in aboveground biomass productivity was of similar amplitude on the three soil types.

1. Introduction

The regulation of the water cycle plays a major role in the functioning of forest ecosystems, especially as it controls the circulation of nutrients between the atmosphere, the soil and the plants. Incident precipitation is partly intercepted and retained by the forest canopy, then partly or fully evaporated. Water passing through the canopy reaches the forest floor as throughfall or as stemflow (Aussenac, 1970; Bellot et al., 1999) and replenishes the soil water reservoir, where it can be taken up by the root system, carry nutrients for biomass production and return to the atmosphere via trees transpiration. Thus forest productivity is a composite resultant of climate conditions, water availability and soil nutrients.

However, research on climate change predicts rising air temperature and altered precipitation patterns, resulting in increasing frequency and intensity of summer drought in parts of Central Europe during the upcoming decades (Schar et al., 2004; Rowell and Jones, 2006). The Intergovernmental Panel on Climate Change reports that these changes will have a significant impact on terrestrial ecosystems and natural resources (IPCC, 2014). In particular, global

* Corresponding author.
E-mail address: marie-pierre.turpault@inra.fr (M.-P. Turpault).

http://dx.doi.org/10.1016/j.foreco.2016.12.024
0378-1127/

warming leading to evapotranspiration increase and rainfall decreases may threaten tree vitality and forest biomass productivity in many temperate regions in the future (Bréda et al., 2006; Allen et al., 2010; Lindner et al., 2010; Medlyn et al., 2011; Hlásny et al., 2014). Climate change will affect the terrestrial biosphere primarily through changes in the regional energy balance and associated changes in the water balance. Soil water shortage impacts several steps of water transfer along the soil-tree-atmosphere continuum (Bréda et al., 2006). As a consequence, forest ecologists and managers are debating on the future of European forests and the right choice of tree species for forestry under a drier and warmer climate (Bolte et al., 2009). Some authors discussed the fate of beech forests in Europe (Geβler et al., 2006; Kramer et al., 2010), which play a central role in forest transition strategies (Tarp et al., 2000) as beech (*Fagus sylvatica*) is one of the most representative deciduous tree species in the Northern hemisphere (Fang and Lechowicz, 2006; Bolte et al., 2007).

In 2003, Europe was affected by a particularly intense heat wave associated with extreme drought and a reduction in primary productivity in several forest types in large parts of the continent, including European beech ecosystems (Ciais et al., 2005; Granier et al., 2007; Hentschel et al., 2015). Such severe regional heatwaves may become more frequent in a changing climate (Meehl and Tebaldi, 2004). In that context, the identification of critical factors and a better understanding of their effect on forest ecosystems are decisive. Currently, the response of plant species to environmental factors is increasingly studied and concerns many applications such as modelling ecological niches, mapping distribution ranges and evaluating species abundance, diversity or productivity (Piedallu et al., 2011; Cheaib et al., 2012). For these studies, the availability of accurate environmental descriptors is of major importance.

The distribution and abundance of forest resources are controlled to a large extent by the quantity and seasonality of available moisture (Neilson et al., 1992). Indeed the soil water holding capacity regulates the water supply of soils with normal vertical infiltration and is a key driver in determining the response and resilience of forested areas to extreme climate events. The soil water balance is recognized as one of the most important soil factors for stand productivity in temperate forests, influencing carbon allocation, microbial activity, nutrient cycling, canopy transpiration and carbon assimilation (Bréda et al., 2006; Lebourgeois et al., 2006). The importance of water availability and water deficit on primary production and growth decline has been discussed by many authors (Mun, 1988; Sala et al., 1988; Sampson and Allen, 1999; Granier et al., 2007; Goisser et al., 2013; Huang et al., 2013; Knutzen et al., 2015). Hence, for a given forest, the consequences of both inter-annual variability and long-term changes of climate conditions might vary considerably in function of soil type. As shown on pedological maps of France (Jamagne, 2011), soil types are widely contrasted at a regional scale. It is a challenge for forest managers to consider this spatial variability of soil properties and to adapt forestry practices to the mosaic of soils. However, relevant soil properties such as thickness of the solum, soil texture and stone content are missing on existing forest site maps and are rarely considered to assess the soil water availability (Schwärzel et al., 2009a).

From this angle, our objective was to test two ecological factors that might control the water balance and stand productivity in a homogeneous beech forest ecosystem (same species, tree age and management practices) developed on much contrasting soils:

- soil type: we compared water fluxes and stand growth on three soil types with different physical properties and soil water holding capacities, ranging from a deep and acidic soil to a superficial calcic soil;
- the inter-annual variability of precipitation amount: by using data collected over four years (2012–2015), including the particularly dry year of 2015 (−24% precipitations in 2015), we aimed to determine the impact of water shortage at the annual scale.

2. Methods

2.1. Study site descriptions

The study was carried out in the Montiers beech forest experimental site, which is managed since 2011 jointly by ANDRA (French National Radioactive Waste Management Agency) and INRA-BEF (French National Institute for Agricultural Research). It was designed to test the effect of soil type on biogeochemical cycling (water and elements) in forest ecosystems. The Montiers site is located in northeastern France in the Meuse department (48° 31′ 54″ N, 5° 16′ 08″ E) where the climate is semi-continental. The annual mean precipitation is 1100 mm and the average temperature over the last ten years was 12.6 °C (Météo-France). The state forest of Montiers was initially chosen because it presents, on a restricted surface area, a diversity of soils representative of the region, from acidic and deep soils to calcic and superficial soils, on which grows a mature and homogeneous beech forest stand (same age, species and forest management). The site covers a soil sequence of approximately 73 ha stretched between 340 and 386 m in altitude in the middle of the forested area. The study area has an overall mean slope of 4.25% with southwest exposure.

The geology of the Montiers site consists of two overlapping soil parent materials, an underlying Tithonian limestone surmounted by acidic Valanginian detrital sediments. The calcareous bedrock contains mainly calcium carbonate and a small amount of clay minerals (~3.4%). The calcareous stones in the regolith are surrounded by a weathered layer rich in clays due to decarbonation. The surmounting detrital sediments are complex (silt, clay, coarse sand and iron oxide nodules) as they result from various depositions and cross-stratifications. The soil properties vary along the soil sequence in relation with the thickness of the sediment layer. According to the World Reference Base for Soil Resources (FAO, 2016), the soil types range from Rendzic Leptosol and Eutric Cambisol on the lower part to Dystric Cambisol at the top of the hillslope (Fig. 1). Table 1 presents some physicochemical properties of the three soils. The Dystric Cambisol (soil 1; S1) formed on the Valanginian sediment layer to a depth of 2 m on average and is slightly acidic ($pH_w < 5$ in the upper soil layers). The cationic exchange capacity (CEC) is <6.7 cmolc kg^{-1} in the first 60 cm of the profile and the effective base saturation ranges between 26 and 64% with Ca^{2+} and Al^{3+} being the dominant cations. Due to the complex sedimentary source material, the resulting soil is characterized by some textural and structural heterogeneity with sandy and clayey passages in the lower soil layers. The Eutric Cambisol (soil 2; S2) formed on a shallower sediment layer. The soil water pH is constant in the soil profile ($5.2 \leqslant pH_w \leqslant 5.4$) and the CEC varies between 7.7 and 17.8 cmolc kg^{-1}; the effective base saturation ranges between 59 and 83% with Ca^{2+} being the dominant cation throughout the profile. The general observation of the soil profile indicated some variability in the depth to the calcareous bedrock. The Rendzic Leptosol (soil 3; S3) lies directly on top of the Portlandian limestone. The soil water pH increases with depth from 5.7 to 6 and the CEC ranges between 20 and 25 cmolc kg^{-1}; the effective base saturation is >94% with Ca^{2+} representing almost all of the exchangeable pool. The carbon-to-nitrogen ratio ranged between 9.7 and 16.2 in function of soil depth in the three soils (Table 1). H*umus* type was eutrophic *mull for the Rendzic Leptosol and acid mull for the Dystric Cambisol.*

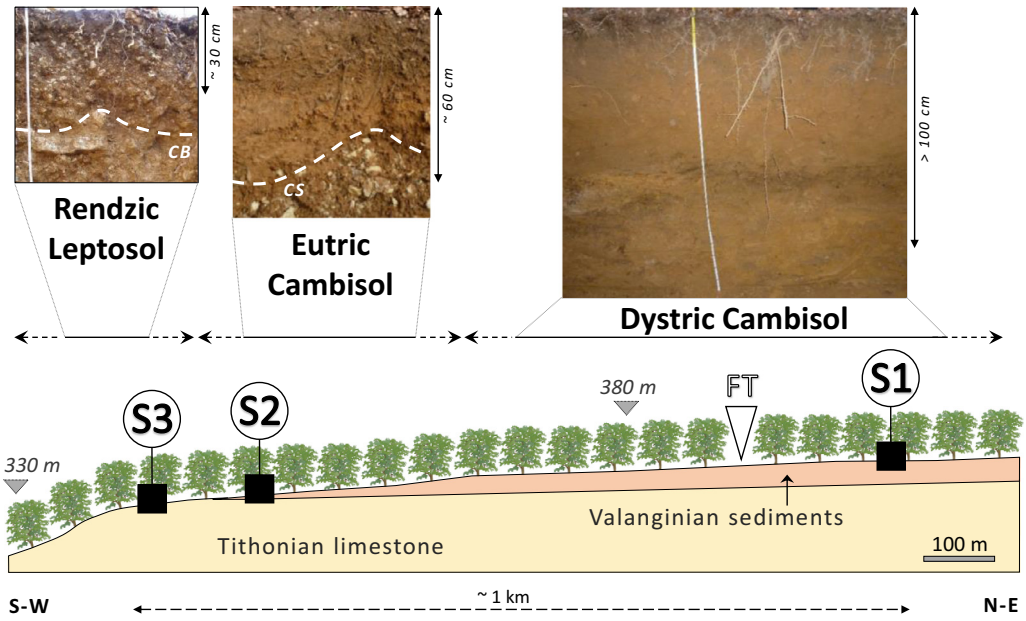

Fig. 1. Geology of the Montiers beech forest experimental site. The black dots represent the contour lines for every 5 m. S1, S2 and S3 represent the positions of the experimental plots. FT, flux tower; S1, S2 and S3 indicate the locations of the three experimental plots; CB, calcareous bedrock; CS; calcareous stones; S-W, south-west; N-E, north-east.

Table 1
Physicochemical properties of the three studied soils in the Montiers site (plot S1 – Dystric Cambisol; plot S2 – Eutric Cambisol; plot S3 – Rendzic Leptosol). Are presented the mean values for bulk density (g.cm^{-3}), textural distribution (g kg^{-1}; clay: <2 µm, fine silt: 2–20 µm, coarse silt: 20–50 µm, fine sand: 50–0.2 mm, coarse sand: 0.2–2 mm), total rock volume (RV), soil water holding capacity (SWHC), soil water pH, organic matter content (OM), cation exchange capacity (CEC; cmol + kg^{-1}) and base-cation saturation ratio (S/CEC, with S = sum of base cations). Standard deviation values are given in italic.

	Depth	B. density	Clay	F. silt	C. silt	F. sand	C. sand	RV	SWHC	pH_{water}	OM	CEC	S/CEC
	cm	g cm^{-3}	g kg^{-1}					%	mm		g kg^{-1}	cmol + kg^{-1}	%
S1 Dystric Cambisol	0–5	0.98	255	281	160	185	121	1.4	8.2	4.9	68	6.7	64
		0.12	*25*	*24*	*17*	*36*	*19*				*22*	*3.0*	*23*
	5–15	0.94	245	276	162	184	131	1.4	16.5	4.8	43	4.2	35
		0.17	*26*	*29*	*17*	*40*	*24*				*16*	*2.2*	*21*
	15–30	1.23	268	280	161	170	115	1.8	22.7	4.8	26	3.5	26
		0.22	*28*	*31*	*21*	*44*	*31*				*9*	*0.9*	*14*
	30–45	1.36	306	262	150	161	119	2.3	22.6	4.9	15	4.3	36
		0.18	*65*	*45*	*27*	*47*	*32*				*5*	*1.6*	*16*
	45–60	1.45	355	229	126	166	141	3.6	18.1	5.1	10	5.7	55
		0.15	*100*	*45*	*31*	*49*	*39*				*2*	*2.6*	*22*
S2 Eutric Cambisol	0–5	1.03	242	242	143	290	83	2.3	9.2	5.4	73	10.1	83
		0.11	*52*	*16*	*13*	*36*	*24*				*26*	*5.4*	*14*
	5–15	0.93	241	246	145	287	82	3.1	18.2	5.2	45	7.8	59
		0.13	*65*	*17*	*13*	*45*	*24*				*29*	*7.3*	*24*
	15–30	1.23	294	234	136	273	64	7.6	19.1	5.3	27	7.7	61
		0.19	*83*	*23*	*17*	*55*	*11*				*13*	*3.9*	*23*
	30–45	1.35	420	188	107	214	71	29.0	14.7	5.3	17	13.2	68
		0.18	*141*	*43*	*31*	*63*	*20*				*8*	*6.9*	*27*
	45–60	1.32	523	154	85	176	63	40.3	10.3	5.4	11	17.8	76
		0.23	*136*	*42*	*32*	*57*	*31*				*4*	*8.8*	*17*
S3 Rendzic Leptosol	0–5	0.88	449	227	123	119	41	2.3	9.8	5.7	109	24.9	98
		0.14	*80*	*54*	*26*	*39*	*15*				*27*	*8.3*	*5*
	5–15	0.98	430	224	114	123	59	4.9	19.2	5.7	71	20.0	94
		0.12	*82*	*56*	*36*	*37*	*21*				*23*	*7.9*	*7*
	15–30	1.06	516	169	77	102	63	36.4	12.5	6.0	42	23.2	99
		0.22	*81*	*50*	*38*	*42*	*24*				*10*	*6.4*	*5*

Three experimental plots were installed along the Montiers soil sequence on each of the studied soil types (Fig. 1): plot S1 (Dystric Cambisol), plot S2 (Eutric Cambisol) and plot S3 (Rendzic Leptosol). Each experimental plot is subdivided into three replicates of 2500 m^2 (total plot surface: 0.75 ha). All nine replicates are equipped with the same monitoring devices designed for the sampling of aboveground and soil solutions, litterfall and tree compartments (stem wood, branches and leaves). The three plots are located on flatter segments of the study area where the slope is nearly equal to zero.

The studied forest is a managed beech high forest. The area has been covered by deciduous forest since at least the beginning of the 19th century. The stand is composed of 89% beech (*Fagus sylvatica*), 6% maple (*Acer pseudoplatanus*) and 5% other deciduous

species: whitebeam (*Sorbus torminalis*), ash (*Fraxinus excelsior*), oak (*Quercus robur*), hornbeam (*Carpinus betulus*) and wildcherry (*Prunus avium*). Stem circumferences at a height of 1.30 m (C130) were measured in 2011 for all trees in each plot; the C130 distribution was very close in the three plots (data not shown). The average age of the trees was 45 ± 7 (S1), 54 ± 3 (S2) and 57 ± 12 (S3) years and the dominant height of the beeches was 26.8 ± 2.2 m. The leaf area index (LAI; leaf cover area in $m^2\ m^{-2}$) was 8.9 in plot S1, 9.4 in plot S2 and 8.7 in plot S3 (data communicated by INRA-EEF). From 2012 to 2015, budburst was observed in late April and leaf fall occurred in November.

2.2. Soil physical properties and vertical root distribution

The variability of the depth to the calcareous bedrock was measured in plots S2 and S3. An excavator was equipped with a 128 cm long graduated metallic rod which was inserted in the soil until the bedrock was reached. Approximately 650 measurements were performed in plots S2 and S3. The proportion of soil volume that was actually occupied by the bedrock (BR) in a given soil layer was measured as follows:

$$BR_X = \frac{\sum_{i=1}^{N_i}[L - D_i] + (N_j \times H_X)}{H_X \times N} \quad (1)$$

where BR_X is the bedrock outcrop ratio in soil layer X (in% of total volume), H_X is the thickness of layer X (in cm), L is the depth of the lower limit of layer X (in cm), N is the total number of measures in the given plot, N_i is the number of measures for which the bedrock resistance was met in layer X, D_i is the bedrock depth of measure i (in cm), N_j is the number of measures for which the resistance was met above layer X.

For each soil type, 27 soil profiles were sampled with an auger in June 2010 following a square grid over the entire plot surface. Soil samples were extracted from each profile following the layers 0–5, 5–15, 15–30, 30–45, and 45–60 cm. All samples were air-dried and sieved at 2 mm before analysis. The soil particle size distribution of the fine earth (<2 mm) was measured by the Laboratory of Soil Analysis of INRA-Arras (France) by sedimentation for clay and silt fractions and sieving for sand fractions (NFX31-107). Bulk density D_b (fine earth dry mass per volume unit) and the ratio of small rock fragments were also measured, with rock fragments being defined as visible mineral fragments >2 mm in size (Tetegan et al., 2011).

In each plot, three soil pits were excavated and soil material was cut and extracted from the pit trenches following the layers 0–5, 5–15, 15–30, 30–45, 45–60 cm and 60–90 cm with 9 replicates per soil layer. In S3, the presence of stones prevented from digging below 30 cm depth. Large rock fragments were removed from the soil material, identified as limestone or iron nodule and independently weighed in situ. Then the large rock fragments content in each soil layer was calculated using the respective density of limestone and iron nodules (evaluated in the laboratory through the buoyancy method) and the soil density (evaluated through the calibrated cylinder method). The total proportion of rock fragments (RF; in% of volume) was defined as the sum of small and large rock fragments. Hence the total rock volume in a given soil layer was calculated as follows:

$$RV_X = BR_X + RF_X \quad (2)$$

With RV_X the rock volume in soil layer X (in%), BR_X the bedrock volume in layer X (in%) and RF_X the volume of total stone fragments in layer X (in%).

The 2D spatial distribution of fine roots (<2 mm in diameter) was quantified through the root impact method. In each plot, the number of root impacts was counted in each square (10 cm × 10 cm) of grids placed in the three pit trenches (>0.5 m distance to the nearest trees). The number of replicates was on average 300 squares per pit trench. For each soil layer, effective root density (RD) was estimated as the number of fine root impacts per dm^2 of trench surface. The vertical root distribution of fine roots within the soil profiles was determined according to the relation:

$$R_X = \frac{RD_X \times H_X}{\sum_{i=1}^{n}[RD_i \times H_i]} \quad (3)$$

With R_X the fine roots proportion in soil layer X (in%), RD_X the density of fine roots in layer X (in root impacts per dm^2 of soil area), H_X the thickness of the soil layer X (in cm) and n the number of soil layers.

2.3. Soil water holding capacity estimation

We used soil water retention curves obtained at different depths in the three soils to determine field capacity (FC) and permanent wilting point (WP) water content. In December 2015 a large soil pit was excavated in each plot and 25 small soil cores (16.5 cm^3 each) were sampled at 10, 30, 60 and 90 cm depth (when possible). In the INRA-BEF laboratory, the samples were fully saturated with deionized water through a capillary system. The samples were placed on a saturated porous ceramic plate inside the pressure extractor (Richards press). Specific pressure was then applied to the samples, allowing water to flow out through the ceramic plate. Five specific pressures were applied on separate samples: −0.01 MPa, −0.033 MPa, −0.1 MPa, −0.33 MPa and −1.5 MPa. For each applied pressure, five soil samples per soil depth and per soil type were used as replicates. When the soil samples reached equilibrium they were removed from the plate and weighed before and after drying at 105 °C to determine the water mass content at each given water potential. Volumetric water content at each applied water potential was calculated for all soil depths as follows:

$$\theta_{p,d} = w_{p,d} \times d_{b,d} \quad (4)$$

where p is the given water potential, d is the soil depth, θ_p is the volumetric water content (in $m^3\ m^{-3}$), w_p is the water mass content (in $kg\ kg^{-1}$) and d_b is the bulk soil density at the depth d.

Water content at field capacity (θ_{FC}) and permanent wilting point (θ_{WP}) in each soil layer were estimated from the water potentials established at −0.01 MPa (pF = 2) and −1.5 MPa (pF = 4.2), respectively. Hence, assuming that stones do not exchange water, the soil water holding capacity (in mm) in each plot was calculated according to the following equation:

$$SWHC = \sum_{i=1}^{n}\left(1 - \left(\frac{RV_i}{100}\right)\right) \times (\theta_{FC,i} - \theta_{WP,i}) \times H_i \quad (5)$$

With $\Theta_{FC,i}$ the volumetric water content at field capacity (in $m^3\ m^{-3}$), $\Theta_{WP,i}$ the volumetric water content at the permanent wilting point (in $m^3\ m^{-3}$), RV_i the rock fraction (in%), H_i the thickness of soil the soil layer i (in m) and n the number of soil layers.

2.4. Climatic data and water sampling on the field

Daily rainfall (P) was monitored by a Météo-France (French national weather service) weather station located in Biencourt-sur-Orge (Meuse, France, station #55051001) at a distance of 4.3 km from the Montiers site. Rainfall was also collected every 28 days on top of a flux tower settled close to plot S1 (45 m above the ground) with four funnel-type polyethylene collectors (0.22 m^2 opening) connected to storage containers (20 L). This device evolved in January 2014 to be replaced with three new collectors

(0.24 m^2) connected to larger containers (50 L). The precipitation amounts collected on the tower were compared to P on a monthly basis. Precipitation during the period of major tree growth (P_{GP}) was determined for each year as the sum of daily rainfall fluxes between bud break and the end of August.

The flux tower was instrumented with micrometeorological and radiation sensors to measure wind speed (Wind Observer 2, Gill, Hampshire, UK), global radiation (CMP21, Kipp&Zonen, Delft, Netherlands), air temperature and relative air humidity (HMP155, Vaisala, Vantaa, Finland) at a daily basis. Potential evapotranspiration (PET) was calculated according to the Penman equation (Penman, 1948).

Under the canopy, throughfall and stemflow solutions were collected every 28 days from January 2012 to December 2015 in the three experimental plots. Throughfall (TF) was sampled in each plot with 12 gutters placed 1.2 m above the forest ground and covering in total 1.56 m^2. The throughfall gutters were distributed in such a way as to integrate the discontinuity of the forest canopy within the plot. Each gutter consisted of a polyethylene funnel-type collector (19.8 cm × 197.8 cm) connected to an underground storage container (120 L). For stemflow (SF) sampling, six trees (15 beeches and 3 trees of another species) of different sizes were selected in each plot. On these trees, SF was collected using flexible polyethylene collars attached horizontally to the stem at 1.50 m height and connected to polyethylene storage containers (120, 150 or 310 L). The trees were chosen so as to represent the different diameter classes in each plot. In winter, SF was collected from 6 trees in each plot and drained into underground storage containers (120 L) to avoid freezing.

2.5. Stemflow and net precipitation

In order to transform the SF volumes to water depth (mm), stem circumference at 1.30 m height (C130) was assumed to explain inter-individual stemflow volume variability within a species (André et al., 2008). Thus all trees in each plot were separated into several C130 classes and the correlation between the SF volume and the C130 was verified for all sampling period. Using the trend line equation, a mean monthly SF volume (V) was then assigned to each C130 class. SF at the plot scale for a given C130 class (in mm) is given by the following equation:

$$SF_z = V_z \cdot \left(\frac{N_z}{A}\right) \quad (6)$$

where z is the C130 class, V_z is the mean stemflow volume per tree in the given C130 class (in L), N_x is the number of trees in the given C130 class and A is the plot area (in m^2).

Total SF at the plot scale was obtained by summing the SF fluxes of all C130 classes. Net precipitation (NP) was defined as the sum TF and stemflow SF water fluxes.

2.6. In situ soil water content measures

Volumetric water content and soil temperature were recorded twice a day and every hour, respectively, by time domain reflectometry (TDR 100, SDEC France) and platinum resistance (Pt100, ACGS Mesure) probes. The TDR system was composed of 2-Rod probes connected to a reflectometer (CAMPBELL Scientific TDR100). Twelve TDR probes per plot and per depth were inserted horizontally at 10, 30, 60 and 90 cm depth (S1), at 10, 30 and 60 cm depth (S2), and at 10 and 30 cm depth (S3). In plots S2 and S3, the placement of the TDR probes was particularly delicate in the soil layers containing a high amount of rock volume; the probes could only be inserted in soil areas that were poorer in rock fragments. Fifteen Pt100 probes per plot were placed at 5, 20, 45, 75 and 105 cm depth (S1), at 5, 20, 45 and 75 cm depth (S2), and at 5, 15 and 45 cm (S3). The volumetric soil water content (θ) was calculated according to the following equation:

$$\theta_{TDR} = a \times (t_m \times f + c \times (20 - T)) + b \quad (7)$$

where θ_{TDR} is the volumetric soil water content (in $m^3\ m^{-3}$), t_m is the measured travel time of the TDR signal along the probe (ns), T is the average temperature measured by the Pt100 probes (°C), f is a probe constant equal to 1.1, *a*, *b* and *c* are coefficients empirically determined through calibration for each soil layer.

The calibration of the TDR probes was performed on soil core samples extracted at each given soil depth in each plot. Linear relationships between θ and the travel time of the TDR signal at constant temperature allowed to determine the coefficients *a* and *b*. The coefficient c was determined from linear relationships between the temperature and the travel time of the TDR signal.

2.7. Water balance model

The conceptual daily water balance model BILJOU©, which main aim is to quantify drought intensity in forest stands, was applied in the three experimental plots to assess the water fluxes and content. A detailed description of BILJOU© is given by Granier et al. (1999). The model uses above-canopy daily measurements of global radiation, air temperature and humidity, wind speed and precipitation. Site-related parameters are: (i) stand canopy phenological parameters: maximum LAI, dates of budburst and complete leaf fall; (ii) soil compartment characteristics: SWHC, θ_{WP}, fine roots distribution, bulk and real density. The model calculates daily water fluxes: trees transpiration (from the Penman equation), rainfall interception, understorey plus soil evapotranspiration and drainage. Resulting day to day variations in extractable soil water content is calculated as follows:

$$\Delta EW = P - I_C - T - ET_U - D \quad (8)$$

With ΔEW the change in extractable soil water content (in mm) between two successive days, P the precipitation, I_C the canopy interception, T the trees transpiration, ET_U the sum of understorey plus soil evapotranspiration and D the drainage at the base of the rooting zone. All water fluxes are expressed in mm. T is subtracted from soil water content in the different rooted soil layers proportionally to the fine roots proportion.

The relative extractable water is calculated daily as follows:

$$REW_t = \frac{EW_t}{SWHC} = \frac{\sum_{i=1}^{n}[EW_{i,t}]}{\sum_{i=1}^{n}[SWHC_i]} \quad (9)$$

where REW_t is the relative extractable soil water on day t (ranging from 0 to 1), $EW_{i,t}$ is the actual extractable soil water in soil layer i on day t (in mm), $SWHC_i$ is the water holding capacity of soil layer i (in mm) and n is the number of soil layers.

Soil water deficit (SWD) was assumed to occur when REW dropped below the threshold of 0.4, inducing stomatal regulation and therefore canopy conductance decline (Granier et al., 1999, 2000b). The duration of soil water deficit (SWD_d) is expressed in number of days for each year.

From daily soil water variations given by BILJOU©, the volumetric soil water content was estimated as follows:

$$\theta_{t,X} = \left(\frac{EW_{X,t} - EW_{X,t-1}}{H_X} \times 100 + \theta_{t-1,X}\right) \quad (10)$$

With $\theta_{t,X}$ the volumetric soil water content in the soil layer X on day t (in $m^3\ m^{-3}$), $EW_{X,t}$ the extractable soil water in layer X on day t given by BILJOU© (in mm), H_X the thickness of layer X (in mm).

For most soil layers the modelled $\theta_{t,X}$ values could be directly compared to the measured θ_{TDR} values. However this comparison

was unfit for the stony layers in S2 and S3 (>15 cm depth), as the TDR probes could only be inserted in soil areas free of stones and bedrock outcrop. Hence, for each stony layer, $\theta_{t,X}$ was corrected for the rock volume by deducing RV from the total soil volume in order to enable the comparison with θ_{TDR}.

Root uptake (RU) in each soil layer was calculated according to the following equation:

$$RU_{X,t} = D_{1,t} - D_{2,t} - (EW_{X,t} - EW_{X,t-1}) \quad (11)$$

where $RU_{X,t}$ is the water uptake by the roots in the soil layer X on day t (in mm), $D_{1,t}$ is the water drainage from the overlapping soil layer (in mm), $D_{2,t}$ is the water drainage at the bottom of layer X (in mm) and $EW_{X,t}$ is the extractable soil water in layer X on day t (in mm).

The contribution of each soil layer to total root uptake was assessed at a weekly time step as follows:

$$\%RU_X = \frac{RU_X}{\sum_{i=1}^{n}[RU_i]} \times 100 \quad (12)$$

With $\%RU_X$ the relative proportion of root uptake in the soil layer X (in%), RU_i the root uptake in the soil layer i (in mm) and n the number of soil layers.

2.8. Stand biomass and growth

In the three plots, tree standing biomass was estimated for each aboveground compartment (i.e. branches <4 cm in diameter, branches between 4 and 7 cm in diameter, branches >7 cm in diameter, wood stem and bark stem) yearly from 2012 to 2015. Allometric equations were used in order to link easily measured tree attributes (i.e. height, diameter at breast height and tree age) to the biomass of each compartment (Picard et al., 2012). The robustness of published models for beech trees in Europe (Genet et al., 2011) was verified thanks to real biomass measurements made on 8 felled beech trees in each plot. These measurements were realized in 2009 following published standards (Henry et al., 2011; Picard et al., 2012), namely by weighting tree compartments and tissues (wood and bark) separately to account for differences in wood density and moisture content. Nonlinear models were used in order to remove the size effect on tree biomass variations and to ensure that heteroscedasticity of biomass data with tree size was taken into account (Saint-André et al., 2005).

Annual aboveground biomass production (BP_A; in tons of dry matter per hectare and per year) was calculated as the difference between the standing biomass of the year n and that of the year n − 1. Water use efficiency (WUE; in t ha^{-1} mm^{-1}) was defined for each year as the ratio of BP_A and annual T.

3. Results

3.1. Soil physical properties and root distribution

In the Eutric Cambisol (S2), the calcareous bedrock appeared on average at 85 ± 8.7 cm depth (data not shown), yet the depth to the bedrock was variable within the plot. As shown in Fig. 2, the bedrock occupied 6% of the prospected ground volume in the 30–45 cm layer and 70% of ground volume in the 90–120 cm layer. Stone fragments made up between 2% (0–5 cm layer) and 45% (60–90 cm layer) of total soil volume. Fine earth reached below 140 cm depth in less than 5% of the prospected S2 area. In the Rendzic Leptosol (S3), the bedrock was reached on average at 44 ± 3.6 cm depth and stone fragments represented between 2% (0–5 cm layer) and 31% (30–45 cm layer) of total soil volume. The prospected volume of the 45–60 cm layer was composed of less than 20% fine earth and below 90 cm depth the bedrock covered 99% of the relative plot surface (Fig. 2). In S1, the proportion of iron nodule stones increased with soil depth, ranging between 1.4% (0–5 cm layer) and 9.3% (150–170 cm layer) of total soil volume.

Fine earth texture varied among the three soil profiles (Fig. 2). S1 was mostly silty (>40%) in the first 45 cm, then the silt fraction (2–50 μm) decreased as the clay fraction (<2 μm) increased. In S2 the silt and sand (0.05–2 mm) fractions were superior to the clay fraction in the 0–30 cm layer (both ranging between 33 and 39%), then they decreased rapidly with depth. In S3, fine earth texture followed the relation clay > silt > sand throughout the profile. The clay fraction increased with depth in all three plots, reaching 72% below −150 cm in S1, 69% below 120 cm in S2 and 71% below −30 cm in S3. The fine silt (2–20 μm) and sand (0.05–0.2 mm) fractions were always superior to the coarse silt and sand fractions, respectively (Table 1). According to the textural classification of the U.S. Department of Agriculture (USDA), the soil texture class varied from loam (0–30 cm) to clay loam (>30 cm) in S1, from loam (0–15 cm) to clay (>30 cm) in S2 and was clay at all depths in S3.

At all depths, fine roots density followed the relation: S3 ⩾ S2 > S1 (data not shown). In the three studied soils, fine roots were mostly located in the upper soil layers and their proportion decreased with depth (Fig. 2). In the rooting zone, 90% of fine roots were observed in the first 30 cm, 45 cm and 90 cm in S1, S2 and S3, respectively. The decrease of root colonization with depth was most pronounced in S1 and least pronounced in S3 (Fig. 2). Less than 1% of total fine roots were located below 100 cm (S1), 160 cm (S2) and 150 cm (S3). Unlike the other two soil types, S3 still presented a relatively high rooting proportion below 45 cm depth (>29% of total fine roots) despite the very low fine earth proportion.

The lower limit of the rooting zone in plot S1 was set at −170 cm where the deepest roots were observed. In plots S2 and S3 their lower limit was respectively set at −140 cm and −120 cm, where the bedrock proportion was ⩽95% of the total ground volume.

3.2. Water holding capacity

The retention curves obtained for the three soil types are presented in Fig. S1. In S3 the volumetric water at field capacity (FC: pF = 2) was constant between −10 and −30 cm depth at ~0.4 m^3 m^{-3} (Fig. S2). On the other hand, the volumetric water content at the wilting point (WP: pF = 4.2) increased from 0.18 m^3 m^{-3} at −10 cm to 0.28 m^3 m^{-3} at −30 cm. In S2, moisture values at FC and WP did not change significantly from −10 cm to −30 cm depth (θ_{FC} = 0.31–0.34 m^3 m^{-3} and θ_{WP} = 0.15–0.17 m^3 m^{-3}) but they increased strongly at −60 cm depth (θ_{FC} = 0.42 m^3 m^{-3} and θ_{WP} = 0.31 m^3 m^{-3}). In S1, FC moisture stayed between 0.34 and 0.36 m^3 m^{-3} along the soil profile, while WP moisture increased steadily from 0.17 m^3 m^{-3} at −10 cm depth to 0.29 m^3 m^{-3} at −90 cm.

As shown in Fig. 2 and Table 1, the soil water holding capacity (SWHC) decreased with depth in all three soil types and ranged between 16 and 8% (S1), 18 and 0.5% (S2), 20 and 0.1% (S3) of total soil volume. The SWHC in the whole considered uptake zone was estimated as 55.5 mm (S3), 83.9 mm (S2) and 204.5 mm (S1).

3.3. Soil moisture dynamics

Soil water content followed the same seasonal dynamics in the three soils and at all depths (Fig. 3). Each year was characterized by a long plateau period of maximum θ (soil saturation; θ_{max}) maintained from winter to the end of spring, followed by a shorter period of soil moisture decreasing to a minimum (θ_{min}) and re-

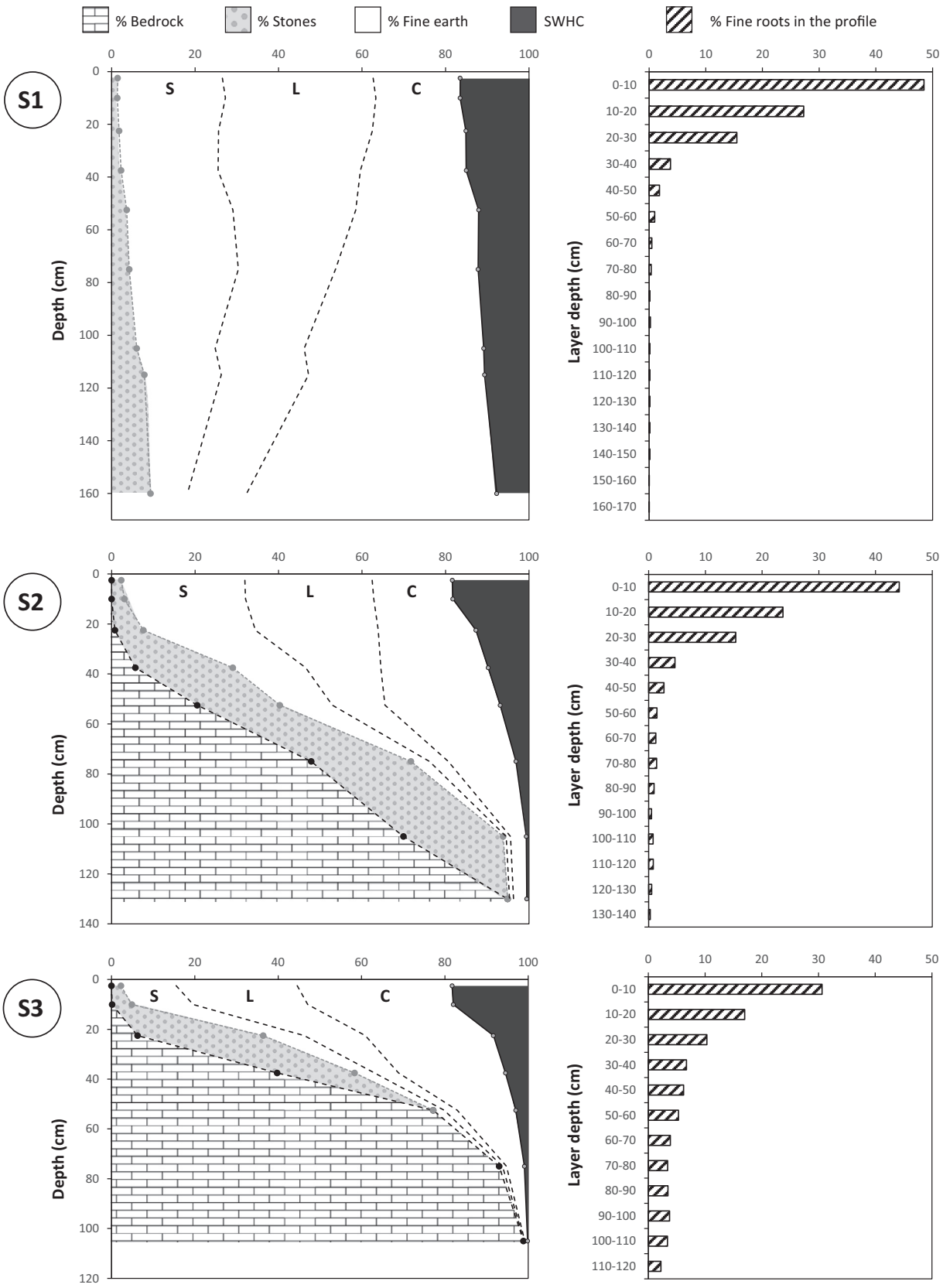

Fig. 2. Physical description of the three Montiers soils (bedrock outcrop, total stones (rock fragments) rate, soil textural distribution, fine roots distribution). The fine earth fraction comprises particles <2 mm in diameter. S1, Dystric Cambisol; S2, Eutric Cambisol; S3, Rendzic Leptosol. S, sand; L, loam; C, clay; SWHC, water holding capacity.

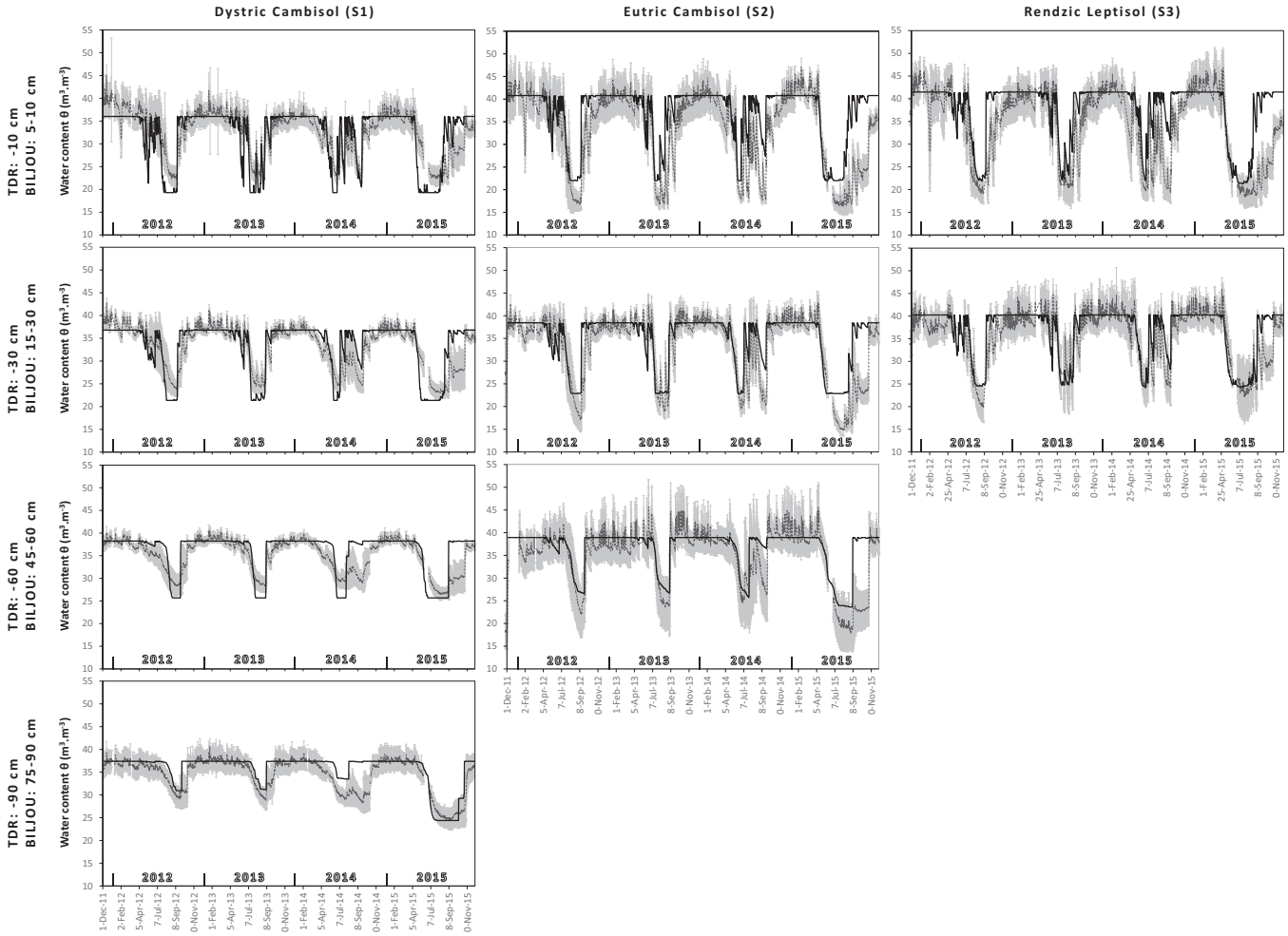

Fig. 3. Daily volumetric water content values measured by TDR probes at −10, −30, −60 and −90 cm soil depth (dashed dark grey line) and estimated by BILJOU© for the 5–10, 15–30, 45–60 and 75–90 cm depth soil layers (solid black line) in the three Montiers soils over the period 2012–2015. For the stony layers in S2 and S3 (>15 cm depth), the BILJOU© estimations were corrected for rock volume in order to enable the comparison with θ_{TDR}. S1, Dystric Cambisol; S2, Eutric Cambisol; S3, Rendzic Leptosol. The light grey areas represent the standard deviations for TDR measurements.

increase during the vegetation period. The amplitude between θ_{max} and θ_{min} generally decreased with depth in all three plots and was lower in S1 than in S2 and S3 (Fig. 3).

In 2012 and 2013 the soil water content decrease began in June-July, while it began at the beginning of May in 2015. In 2014 the decrease was particularly early (end of February–March) in comparison to the other years. In 2012 the minimum was reached in September for a short period of time (less than 15 days) and in 2013 θ_{min} was maintained from August to the beginning of September. In 2014, the minimum was met during two short periods (June-July and beginning of October) separated by a water content rebound in August. In each soil type and at a given depth, water volumetric content at the minimum was very similar from 2012 to 2014, except in S3 at −30 cm where θ_{min} was lowest in 2012 (Fig. 3). In 2015 (driest year) the soil moisture minimum was maintained for a longer period, from July to September, in all three plots. Furthermore, θ_{min} was lower in 2015 than in the previous years at all depths, except −10 cm in S1 and S2. Following the soil water re-increase in autumn, the field capacity recovered again in December (in 2012 and 2014) or October-November (in 2013). In 2015 the recovery was slower, passing by an intermediate plateau in October-November, and θ_{max} was reached later (December-January) than in the previous years.

Along the soil profiles, the water content decrease in spring/-summer was noticeably delayed in time with increasing soil depth. In particular in 2014, the decrease at −60 cm (in S2) and −30 cm (in S3) occurred approximately 1 month later than in the upper soil layers (Fig. 3). This delay effect could not be observed in 2015, as during that dry year soil moisture decreased simultaneously along the whole profile in all three soils. The reverse phenomenon was evidenced in autumn/winter in S2 and S3: the saturation point was generally reached slightly sooner in deeper soil layers than in the surface layer (Fig. 3). In S1, however, the water content re-increase seemed to occur simultaneously at all depths (Fig. 3).

3.4. Water balance modelling results

3.4.1. Modelled aboveground fluxes and soil water transfer

Fig. 4 shows monthly precipitation measured at the nearby meteorological station and both net precipitation estimated by BILJOU© and measured in Montiers over the period 2012–2015. Mean annual precipitation over the study period was 1090 ± 191 mm year^{-1} (Table 2), the wettest year being 2013 (P = 1338 mm) and the driest year being 2015 (P = 875 mm). There was a good correlation between modelled and measured net precipitation (R^2 = 0.95). Measured mean annual canopy interception was close in the three plots as they exhibited similar leaf area index: 183 ± 17 mm (plot S1), 183 ± 21 mm (S2) and 202 ± 20 mm (S3).

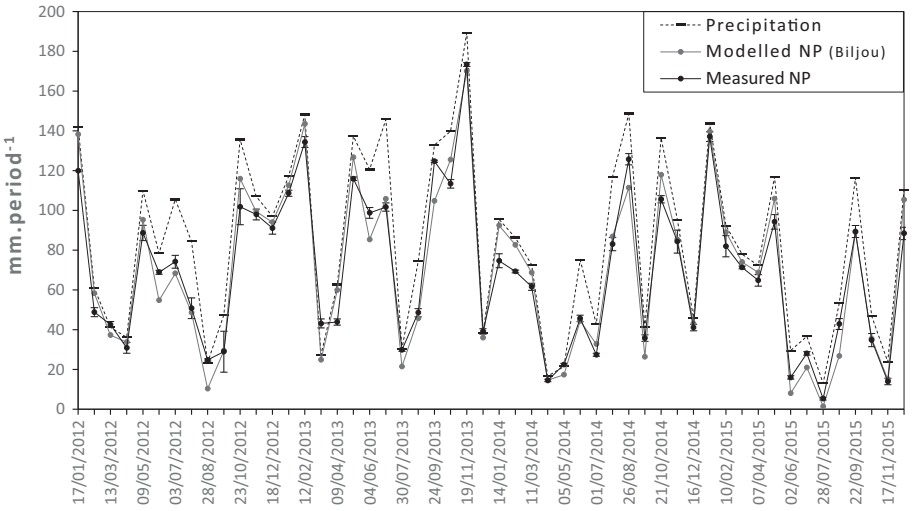

Fig. 4. Monthly precipitation and net precipitation (NP) in mm per period of 28 days over the studied years 2012–2015. Precipitation was measured at the meteorological station of Biencourt-sur-Orge (at a distance of 4.3 km from the Montiers site). Modelled NP is estimated by BILJOU©; measured NP is the sum of measured throughfall and stemflow.

Table 2
Measured and modelled annual water fluxes (in mm), soil water holding capacities (SWHC), soil water deficit duration (SWD_d) and aboveground biomass production (BP_A) in each plot during the studied period (2012–2015). S1, Dystric Cambisol; S2, Eutric Cambisol; S3, Rendzic Leptosol. P, annual precipitation; P_{GP}, precipitation during the principal growing period (from bud break to the end of August); NP, net precipitation; SF, stemflow; I_C, canopy interception; T, trees transpiration; ET_U, understorey evapotranspiration; D, drainage; SD, standard deviation.

Plot	Year	Measured						Modelled (Biljou)						Stand growth
		P	P_{GP}	NP	SF	I_C	SWHC	NP	I_C	T	ET_U	D	SWD_d	BP_A
		mm year^{-1}					*mm*	*mm year^{-1}*					*days*	*t ha^{-1} year^{-1}*
S1	2012	1095	369	891	43	179	205	909	186	344	34	542	17	10.8
	2013	1338	462	1172	53	192	205	1138	201	330	30	790	13	10.8
	2014	1017	427	795	33	201	205	846	172	330	34	492	0	10.6
	2015	875	270	773	38	161	205	723	152	292	34	408	80	7.8
	Mean	1081	382	908	42	183		904	178	324	33	558	28	10.0
	SD	*194*	*84*	*184*	*9*	*17*		*174*	*21*	*22*	*2*	*164*	*36*	*1.4*
S2	2012	1095	369	869	46	200	84	904	191	281	34	592	46	8.7
	2013	1338	462	1182	57	183	84	1135	203	263	30	843	57	8.5
	2014	1017	427	801	35	194	84	843	174	286	34	527	28	8.2
	2015	875	270	779	41	154	84	719	155	191	34	497	110	6.3
	Mean	1081	382	908	45	183		900	181	255	33	615	60	8.0
	SD	*194*	*84*	*187*	*9*	*21*		*174*	*21*	*44*	*2*	*157*	*35*	*1.1*
S3	2012	1095	369	849	43	221	56	912	183	259	35	618	60	6.1
	2013	1338	462	1173	53	191	56	1139	200	241	31	867	58	6.8
	2014	1017	427	778	32	217	56	847	170	264	35	548	39	5.9
	2015	875	270	753	38	180	56	724	150	172	35	517	113	4.2
	Mean	1081	382	888	42	202		906	176	234	34	638	68	5.7
	SD	*194*	*84*	*194*	*9*	*20*		*174*	*21*	*42*	*2*	*159*	*32*	*1.1*

The comparison of modelled daily soil water content (BILJOU©) and in situ TDR measurements at different depths over the period 2012–2015 is presented in Fig. 3. In S1, the modelled extractable water (EW_{Biljou}) was slightly higher than the extractable water derived from TDR measurements (EW_{TDR}) at −10, −30 and −60 cm depth (Fig. 3). In S2, on the contrary, EW_{Biljou} was lower than EW_{TDR} at all depths during the whole study period. In S3, EW_{Biljou} and EW_{TDR} were equal at all depths.

In the three soil types and at all depths, modelled soil moisture followed the same dynamic as TDR measures, except certain divergences described hereafter. Regarding S1, BILJOU© predicted a faster soil moisture decrease in summer 2012 and spring 2015 at all depths as compared to in situ θ measurements (Fig. 3). The second θ minimum of the 2014 vegetation period, observed after the rebound of July-August, was less pronounced in the model predictions than according to TDR measures; at −60 cm the model indicated no second moisture decrease at all. Lastly, the model predicted a much faster soil moisture increase at the end of the 2015 minimum plateau in all three soil types and at all depths; field capacity was reached at the end of September 2015 (Fig. 3).

REW was below the transpiration regulation threshold (REW < 0.4) for an average of 28 (S1), 60 (S2) and 68 (S3) days year^{-1} over the period 2012–2015 (Table 2). Water deficit duration (SWD_d) was shortest in 2014, lasting for 28 and 39 days in S2 and S3, respectively (Figs. S3b and S3c). In S1, REW stayed above the 0.4 threshold in 2014 (Fig. S3a). On the contrary, soil water deficit lasted for a particularly long time in 2015: 80 days (S1), 110 days (S2) and 113 days (S3). In July-August 2015, REW even dropped below 0.1 for >40 days in S2 and S3 (Figs. S3b and S3c).

Modelled annual drainage below the rooting zone (D) was well correlated with annual precipitation ($R^2 = 0.9$) and increased

slightly from S1 to S3; according to years, D ranged between 408 and 790 mm (S1), 497 and 843 mm (S2), 517 and 867 mm (S3).

3.4.2. Root water uptake

Time courses of T, REW and root uptake proportion in the different soil layers (%RU) during the period 2014–2015 are presented in Fig. S3 for the three plots. The trees transpired throughout the vegetation periods, but T was strongly limited in 2015 when REW was below 0.1. Mean annual T estimated by BILJOU© was 324 ± 19 mm year^{-1} (plot S1), 255 ± 38 mm year^{-1} (plot S2) and 234 ± 37 mm year^{-1} (plot S3). Annual T was negatively correlated with the soil water deficit duration (SWD_d) in all three plots (R^2 = 0.8).

According to the model estimations, ~90% (S1), ~85% (S2) and ~65% (S3) of RU took place in the 0–30 cm soil layer when REW ~ 1. In S1 and S2, when REW decreased below 0.4, %RU dropped rapidly to 0 in the surface layer and water uptake took then successively place in the underlying layers (Fig. S3). In S1, when %RU dropped in the surface layer, water uptake first took place in the 30–60 cm layer (up to% RU ~ 70%), then in the 60–90 cm and 90–170 cm layers (up to %RU ~ 50% and >40%, respectively); during the dry period of 2015, RU occurred almost exclusively in the 90–170 cm layer (Fig. S3a). In S2, the 30–60 cm layer was the main uptake source when %RU dropped in the surface layer (Fig. S3b); in July 2015 when REW < 0.1, up to >80% of RU took place in the 30–60 cm layer. The underlying soil layers of S2 supplied up to ~30% (60–90 cm) and ~7% (90–140 cm) of RU. In S3, RU followed a different pattern: when REW decreased, %RU instantly increased in the surface layer and decreased in the underlying soil layers (Fig. S3c). Consequently, when REW < 1 water uptake took place almost entirely in the 0–30 cm layer (60 < %RU < 100%), and to a lesser extend in the 30–60 cm layer (0 < %RU < 25%); in 2015, during the soil water deficit period from mid-June to mid-September, the model estimated that all water uptake occurred in the surface layer.

3.5. Stand growth versus water balance and soil water deficit

Annual aboveground biomass production in each plot and for each year of the study is given in Table 2. BP_A was highest in plot S1 and lowest in plot S3 each year of the study period. In each plot, annual biomass production was nearly the same from 2012 to 2014 (10.7 ± 0.1 t ha^{-1} in S1; 8.5 ± 0.2 t ha^{-1} in S2; 6.3 ± 0.5 t ha^{-1} in S3), but it was significantly lower in 2015 (7.8 ± 0.6 t ha^{-1} in S1; 6.3 ± 0.9 t ha^{-1} in S2; 4.2 ± 1 t ha^{-1} in S3).

Likewise, annual trees transpiration (T) was constant from 2012 to 2014 in each plot: 335 ± 8 mm in S1, 277 ± 12 mm in S2 and 255 ± 12 mm in S3. In 2015, T decreased by 13% (S1), 31% (S2) and 32% (S3) compared to the three previous years. Each year, annual T was perfectly correlated with SWHC when comparing the three plots (R^2 > 0.97; data not shown).

Fig. 5a presents the comparison between annual aboveground biomass production and precipitation during the vegetation period (P_{GP}). The more productive years 2012–2014 were characterized by P_{GP} values ranging between 369 and 462 mm. The year with lower biomass production (2015) had less precipitation during the vegetation period (P_{GP} = 270 mm).

As shown in Fig. 5b, a good correlation was evidenced between the annual aboveground biomass production and annual trees transpiration (R^2 = 0.8) when considering all three plots and all years from 2012 to 2015, in accordance to the following linear regression equation:

$$BP_A = 0.036 \times T - 1.97$$

We confronted this result with data collected in another beech forest experimental site located in Hesse (Moselle, northeastern France). The annual T and BP_A values measured for the Hesse stand fit perfectly on the regression line of the above given relation (Fig. 5b).

4. Discussion

4.1. Soil physical properties spatial variability

Along the ~1000 m long Montiers soil sequence, under the same climate, soil physical properties evolved importantly in relation with the underlying bedrocks. From hilltop over detrital sediments to the lower part over limestone, soil depth decreased, the clay-sized fraction of fine earth increased and the stone fragments proportion increased. These differences led to highly contrasting water holding capacities. The size of the fine earth reservoir, i.e. depth to the bedrock and amount of stones along the profile, was the primary factor that determined the size of the available soil water reservoir. Thus the Dystric Cambisol (S1), with ~2 m thickness, had a soil water holding capacity >200 mm; in comparison, the SWHC of the intermediate Eutric Cambisol (S2) was less than half as high. On the other hand, the shallow Rendzic Leptosol (S3) had a SWHC of only 56 mm, even when taking into account the water contained in the saprolite layer.

Granier et al. (2000a) and Schwärzel et al. (2009b) demonstrated that the spatial variability in soil water content under

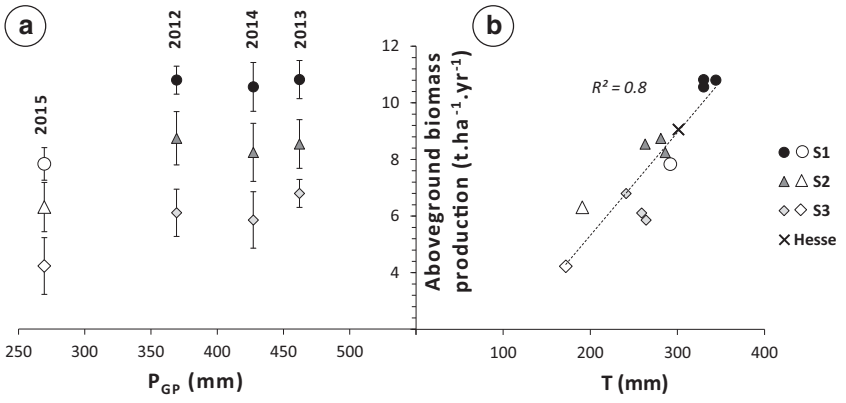

Fig. 5. (a) Relationship between annual aboveground biomass production (BP_A) and cumulated precipitation amount during the vegetation period (from bud break to the end of August; P_{GP}) for each year of the study (2012–2015). (b) Relationship between BP_A and trees transpiration (T) in the three Montiers plots (for each year of the study) and in the Hesse experimental site (Moselle, France). S1, Dystric Cambisol; S2, Eutric Cambisol; S3, Rendzic Leptosol. The larger white symbols stand for the drier year 2015.

beech was mainly due to differences in soil properties and root intensity. In Montiers, water content at the wilting point increased with increasing clay content; so did water content at field capacity, but to a lesser extent as this tendency was limited by increasing density with depth. Thus the high clay amounts in S3, leading to less extractible water, was counterbalanced by lower soil bulk density in S3 than in S1 and S2. In overall, fine earth textural distribution and bulk density did not contribute much to the SWHC differences between the three soils. These results show that important variations of soil water reservoirs exist even on the scale of a small water catchment. In an overview by Piedallu et al. (2011) of >100,000 forest plots recorded in France within the framework of forest inventories, SWHC ranged between 0 and 148 mm for soil down to a depth of 1 m, with an average of 78 mm and important variations on a local scale. In southeastern United States, estimates of available water holding capacity by Sampson and Allen (1999) from a natural resource conservation soils database gave median SWHC values that varied from 100 to 250 mm across the forest type for a normalized 1.25 m soil profile. Unfortunately, in these two studies, SWHC was not evaluated according to fine root depth, i.e. it did not inform on the total extractable soil water for trees.

When determining the water uptake zone, two specific cases were met in the Montiers site: a thick soil in which roots did not reach the consolidated bedrock (S1) and shallower soils in which root colonization extended to the limestone bedrock (S2) and even further (S3). In S3, fine roots were observed directly in the limestone bedrock, growing in cracks and through the rock. We highlighted considerable differences in maximum rooting depth and root biomass distribution among the three soil types, which certainly affect the ecosystem's functioning. Indeed the plant rooting depth influences the hydrology, biogeochemistry and primary productivity of terrestrial ecosystems (Jackson et al., 1999). In absence of stones and bedrock in the uptake zone, the fine roots system was superficial in S1, with 90% of roots in the first 30 cm (Fig. 2). As a comparison, Schwärzel et al. (2009b) observed in a beech stand in eastern Germany that even though the beech had roots down to a depth of 80 cm, 90% of the fine roots were concentrated in the upper 40 cm of the soil. In S2 and, even more, in S3 the root system was more evenly distributed despite the high stone proportion in the uptake zone. These differences in rooting profiles manifest the plasticity of beech trees. Significant amounts of stone volume in the shallow layers might oblige roots to grow deeper. In addition, fine roots biomass was highest in S3 and lowest in S1, which could be explained by soil base saturation differences. Another explanation for higher root biomass and deeper prospection in S3 could be the allocation of root biomass to the underground tree compartment in order to increase prospection and water uptake in response to a low soil water holding capacity. Although root biomass generally decreases with depth in the soil (Gale and Grigal, 1987), plants show great flexibility in allocating roots and adjusting resource uptake in layers with high resource availability (Jackson et al., 1990; Robinson, 1996; Fransen et al., 1998; Turpault et al., 2009). As shown by Knutzen et al. (2015), plant morphology and in particular root growth can respond to reduced water availability with higher phenotypic plasticity. Increasing root/shoot ratio and rooting depth with decreasing water availability was also highlighted by Goisser et al. (2013) in a juvenile beech stand. The ability of some plants to grow roots into the underlying bedrock, as observed for S3, is already known (Lewis and Burgy, 1964; Zwieniecki and Newton, 1995; Jackson et al., 1999; Estrada-Medina et al., 2012). We may suppose that the actual maximum rooting depth in S3 exceeds the considered 120 cm depth, thus slightly increasing the estimated SWHC. Canadell et al. (1996) gave a mean maximum rooting depth value of ~2.9 m for temperate deciduous forests.

4.2. Comparison between modelled and measured soil water content

The variability of θ measurements among TDR probes placed at a same depth showed that soil water content varied noticeably at the plot scale. This confirms the necessity of placing a sufficient number of soil water sensors within the plot, covering the variability of soil properties, to get a representative image of soil moisture. Small-scale variability of soil hydraulic properties and θ within apparently homogeneous sites has been shown in previous studies (Bouten et al., 1992; Schwärzel et al., 2009b).

The differences between the amount of extractable water measured from TDR measurements and derived from the BILJOU© model in S2 (Fig. 3) are most probably due to the fact that the TDR probes were inserted in soil areas free of stones, which correspond to deeper soil conditions and are thus not representative of the total given soil layer. The soil physical properties in such areas may differ from the mean soil layer characteristics used for the modelling, inducing differences in the soil water holding capacity. In situ observations showed in particular that the amount of clay tended to be lower in the deeper soil areas where the TDR probes were inserted.

Overall the TDR measurements and the model predictions followed very similar daily soil moisture variations. The biggest difference between modelled and measured moisture dynamic was put into evidence at the end of the long dry period of 2015; fine earth rewetting took longer than predicted by the model in all three soils. This might be due to soil desiccation and cracks formation as a consequence of prolonged drought conditions, leading to preferential flow and delaying the refilling of the water reservoir, which phenomenon not being well-reproduced by the model. Else BILJOU© gave an accurate transcription of moisture dynamic, aside from minor offsets in SWHC emptying speed in S1 and the moisture rebound in the middle of the 2014 vegetation period which could not be predicted efficiently by the model.

4.3. Effect of soil type on the water balance

The soil water reservoir emptying and refilling dynamics were very similar in the three plots, despite the differences in soil physical properties (density, texture). Mean annual soil water deficit duration (SWD_d) was strongly positively correlated to SWHC. The longest water deficit duration was experienced in the 2015 in all plots. SWD_d was not only dependent on total precipitation amount during the vegetation period (P_{GP}), but also on the distribution of rainfall during that period. In all three plots, SWD_d was lowest in 2014, during which year rainfall was particularly low from budbreak to June (140 mm) but much higher from July to August (287 mm) compared to the other three years (data not shown). In some forests, T is decreased during periods of limited water availability as a consequence of canopy stomatal conductance reduction (Oren et al., 1998; Bréda et al., 2006; Köcher et al., 2009). However, Schwärzel et al. (2009b) observed no reduction of transpiration following water shortage with REW < 0.4 in a beech stand. Likewise, Oishi et al. (2010) measured no T reduction in an oak stand during a severe drought year. In our study, there was a reduction of T in all three plots in 2015 with SWD_d being equal or longer than 80 days and it was particularly marked when SWD_d exceeded 100 days. Such a T reduction manifests down-regulation processes that occur when the root uptake of remaining available water requests highly negative suction potentials (Bréda et al., 1995). Yet when P was above 1000 mm yr^{-1}, inter-annual variation of T was very low in the three plots.

Observation of soil water dynamics can provide an insight into the water supply for plants during the growing season (Bréda et al., 1995). When the soils were close to field capacity, root uptake took

place in the upper soil layer (first 30 cm) in the three plots. Whereas during the vegetation period, root uptake followed two different patterns depending on soil type and fine roots distribution. In S1 and S2, soil water uptake showed a gradual downward shift as the soils became drier. During drought periods (REW < 0.4), water uptake took mostly place in the 90–170 cm layer (S1) and in the 30–60 cm layer (S2). Layers below 60 cm depth in S1 contributed much less to root uptake as they were characterized by low water holding capacity due to high stone and bedrock rates. Schwärzel et al. (2009b) and Granier et al. (2000a) also demonstrated that the deeper soil layers significantly contributed to the overall evapotranspiration of a beech stand when the soil became drier, in eastern Germany and eastern France respectively. On the other hand, in S3 water was still taken up almost exclusively in the surface layer (0–30 cm) during drought periods, which underpins the importance of occasional rain events during such periods of water shortage for providing limited water supply in shallow soil conditions. According to Bréda et al. (1995) and Bréda et al. (2006), deep roots (<1 m depth) contribute to 90% of tree water alimentation during extreme dry events. Yet our results show that the root uptake pattern during water shortage periods depends strongly on soil type. Deep roots in S3 probably have an importance for nutrient supply, organic matter in cracks and fissures within the rock being a possible source of additional nutrients for the trees, but were of low importance for water quantitative uptake. Göransson et al. (2008) showed that fine roots with different physiological properties at different soil depths could control the nutrient uptake of trees. Furthermore the mycorrhizal communities change with soil depth (Rosling et al., 2003), which might also influence nutrient uptake capacity at different soil depths. These statements may be of importance when estimating the impact of dry years on the total nutrient uptake.

Net precipitation and canopy interception were very similar in the three plots (Table 2) as a result of similar leaf area index values, which indicates that the three soils were replenished with the same amount of water at the yearly scale. The plots differed in trees transpiration (S1 > S2 > S3) and drainage at the bottom of the uptake zone (S1 < S2 < S3). Thus actual evapotranspiration was higher for the stand in plot S1, while loss to the groundwater system was higher in plot S3 (Table 2).

Schipka et al. (2005) studied the regional variability of T in Central European beech stands with a meta-analysis approach. They noted a mean annual trees transpiration of 289 ± 58 mm and described a humped-shaped relationship between T and annual precipitation (P), with a broad transpiration maximum in the P range between ~700 and 1000 mm yr^{-1} (which may indicate T limitation for P < 700 mm yr^{-1} and reduced T for P > 1000 mm yr^{-1}). Considering that in Montiers mean annual P was slightly past the given maximum level limit (P = 1080 mm yr^{-1}), the stand growing in plot S1 transpired more (mean T = 324 mm yr^{-1}) while the stands in plots S2 and S3 transpired slightly less (255 and 234 mm yr^{-1} respectively) than predicted by Schipka et al. (2005). We concluded that the soil water reservoirs must be taken into account when analyzing the relationship between P and T.

4.4. Stand growth depends highly on the water balance

Despite large differences in SWHC among the three soils, beech stand productivity was in the highest class according to beech yield classes established in north-eastern France (Decourt, 1973; Seynave et al., 2008) and measured leaf area index (LAI) values were similar in the three plots. In regard of the superficial root system in S1, trees certainly found enough water and nutrients in the superficial soil layers to sustain the productive stand. The beech stand was productive on S3 despite very low soil water holding capacity and minor importance of deep roots for quantitative water uptake. This confirms the efficiency and importance of sufficient rain events during the vegetation period on a shallow soil. Indeed the climate determines the relative importance of water or nutrition on forest growth (Sampson and Allen, 1999). There was a mean aboveground biomass production level relative to each soil type during the three wet years 2012–2014 (Fig. 5a) in that order: plot S1 (10.7 ± 0.1 t ha^{-1} yr^{-1}) > plot S2 (8.5 ± 0.2 t ha^{-1} yr^{-1}) > plot S3 (6.3 ± 0.5 t ha^{-1} yr^{-1}). Thus BP_A increased with increasing SWHC (R^2 = 0.9). Some authors also found that low water availability can lead to lower primary production, via experimentation (Mun, 1988; Goisser et al., 2013; Knutzen et al., 2015) and modelling approach (Sampson and Allen, 1999; Huang et al., 2013) and data analysis (Sala et al., 1988), confirming the importance of water availability as a control on stand production. Bréda et al. (2006) states that variations in water availability account for up to 80% of the inter-annual variability in biomass increment in temperate stands. Piedallu et al. (2011) observed that SWHC explained ~10% of the height growth index variance for beech in a meta-analysis grouping French plots (n = 866). Our study puts into evidence a strong control of SWHC over tree productivity at a very local scale within a same beech stand.

In the three plots BP_A dropped in the dry year 2015 by approximately 29 ± 4% compared to the three previous years. We speculate that there is a P_{GP} threshold between 270 and 370 mm below which tree growth in Montiers is negatively impacted through soil water deficit affecting root water uptake and beech transpiration. Using the BILJOU© model, Granier et al. (2007) showed that beech growth decline was directly related to soil water deficit intensity. Despite higher water deficit experienced in plots S2 and S3, the BP_A reduction in 2015 was similar in the three plots. Thus the prolonged water shortage situation seemed to impact the stands growing on the three soil types with the same intensity. However this study only concerns a single dry year; this conclusion clearly cannot be generalized to a long series of drought years. A negative impact of drought on the stand may also be delayed in time, as clearly demonstrated by dendrochronological studies (Granier et al., 1999; Lebourgeois et al., 2005). Power (1994) also mentioned twig growth reduction over several years after drought for beech.

Under a given climate and similar stand conditions, transpiration seemed to be the evident primary driver of aboveground biomass production, since BP_A was correlated to trees transpiration when considering the three plots together (Fig. 5b). Mass flow is defined here as the transport of soil solution (water and nutrients) along the water potential gradient driven by transpiration. This BP_A/T correlation was surprising given the major differences in soil properties and questioned the existence of secondary drivers of productivity such as the soil nutrient level. In Douglas-fir and red alder stands, Moore et al. (2011) highlighted that, instead of more productive stands transpiring more, the greatest variability in both productivity and T was determined by site conditions. This was not the case in Montiers; we raised two possibilities:

- Either mass flow was the only significant driver in Montiers, which would imply that there was no limiting nutrient in any of the three soil types;
- or tree adaptations to soil conditions such as physiological plasticity, fungal associations and/or root interception of nutrients (active growth towards sources of nutrients) compensated for eventual nutrient deficits, thus reducing the impact of the soil fertility level.

Despite the general BP_A/T correlation, a more detailed comparison of the relationship between transpiration and biomass increment among the plots showed that water use efficiency was

significantly lower in plot S3 (WUE = 0.025 ± 0.002 t ha^{-1} mm^{-1}) than in plots S1 and S2 (WUE = 0.031 ± 0.002 t ha^{-1} mm^{-1}). This implies that a secondary factor, less important than the water availability and linked to soil type, controls stand productivity in Montiers. According to Moore et al. (2011), lower soil fertility reduces net primary production while maintaining higher transpiration, thus reducing the water use efficiency (WUE). Likewise, Fernández-Martínez et al. (2014) states in a synthesis study that in nutrient-poor forests a much larger proportion of gross primary production is released through ecosystem respiration, resulting in lower carbon-use efficiency. Surprisingly, the level of soil exchangeable nutrients obviously did not explain the WUE differences in Montiers as S3 had similar or higher base cation concentrations in the soil solutions compared to the other soil types (data not shown). Thus, in our site, soil fertility was not a significant driver of stand productivity in the context of major water availability differences among plots. One explanation for the lower WUE in S3 could be the existence of a SWHC threshold level below which the tree physiology is impacted. Water deficit duration did not seem to control the stand productivity of the same year in Montiers as the WUE did not decrease with increasing SWD_d in a same plot when comparing the four vegetation periods; in particular the WUE was not significantly different in 2015 than the previous years. However this observation cannot be generalized to longer drought periods.

5. Conclusions

Our study shows that soil type is a major driver of the water cycle and stand growth, primarily through its soil water holding capacity. Under a given climate and with stand, site exposition and solar radiation continuity, stand biomass production and trees transpiration was positively correlated with the soil water holding capacity. SWHC, annual T and BP_A increased along the Montiers soil sequence in that order: Rendzic Leptosol < Eutric Cambisol < Dystric Cambisol. These results imply that, within a forested area composed of a mosaic of different soils, the water balance and the vegetation growth potential vary according to soil properties, especially the depth to the bedrock and the rooting depth. Secondly, precipitation level during the vegetation period also impacted stand growth, but only below a certain threshold of low rainfall (P_{GP} between 270 and 370 mm). Above that threshold, annual stand biomass increment was not directly related to P_{GP}. During the drier year 2015, the decrease in aboveground biomass productivity was of similar amplitude for the stands growing on the three soil types.

However these two factors, soil type and precipitation, followed the same rule which is that trees transpiration strongly controlled stand growth. This relation was confirmed by the comparison of our results with a second beech forest experimental site located in northeastern France. Thus the amount of water taken up by the roots and transpired from the canopy seems to be the main driver of stand productivity in beech forests in temperate regions. Small differences in water use efficiency and response to water shortage among the three studied soil types might indicate the influence of one or several secondary factor(s) impacting stand productivity, such as soil nutrient availability. Stand adaptation processes to environmental conditions, such as physiological plasticity, fungal associations, root specialization and/or root interception of nutrients, probably reduced or even compensated for secondary drivers of stand productivity.

Given the geological complexity in Europe, situations of contrasting soils at a regional scale are very frequent. As shown by our findings, a significant issue for forest managers could be to further adapt forestry practices to management units based on soil physical properties. However the actual layout pattern of forest plots in France is often independent from the spatial distribution of soil types; this is particularly the case in the studied area of Montiers. Thus the same forest management planning may be applied to stands growing on soils characterized by very different physico-chemical properties (notably physical properties that control the soil moisture regime). In view of these observations, an important measure towards a site-adapted and sustainable management of forests would be the modification of the forest cadaster by taking the distribution of soil types into account. In parallel, soil maps should be completed with accurate information about major physical soil properties such as the depth to the bedrock.

In order to anticipate the long-term effect of water shortage and test the limits of stand adaptation mechanisms, longer forest studies cumulating data over successive drought episodes are needed. In particular studies simulating water deprivation, notably through rain exclusion using roofs under the forest canopy, might contribute to understanding the possible impact of climate change on forest ecosystems. To assess a potential effect of the soil nutrient level on T and BP_A, it would be necessary to realize tests of nutrient manipulation, in the same context of equivalent climate and stand conditions.

Acknowledgements

The authors would like to thank the technical staff of INRA-BEF and ANDRA for field sampling, and in particular Serge Didier as technical manager of the Montiers site. We are particularly grateful to Claire Pantigny and Maximilien Beuret for the numerous solutions analyses. We are also grateful to Météo-France for the communication of meteorological data and to Bernard Longdoz and Laura Heid (INRA-EEF) for the communication of LAI values. We thank ANDRA, INRA, GIP Ecofor and AnaEE France for the financial functioning of the Montiers site, and ANDRA for financing Gil Kirchen's doctoral thesis. We would like to acknowledge the National Forest Office (ONF) for welcoming us into the domanial forest of Montiers.

Appendix A. Supplementary material

Supplementary data associated with this article can be found, in the online version, at http://dx.doi.org/10.1016/j.foreco.2016.12.024.

References

Allen, C.D., Macalady, A.K., Chenchouni, H., Bachelet, D., McDowell, N., Vennetier, M., Kitzberger, T., Rigling, A., Breshears, D.D., Hogg, E.H., Gonzalez, P., Fensham, R., Zhang, Z., Castro, J., Demidova, N., Lim, J.-H., Allard, G., Running, S.W., Semerci, A., Cobb, N., 2010. A global overview of drought and heat-induced tree mortality reveals emerging climate change risks for forests. For. Ecol. Manage. 259, 660–684.

André, F., Jonard, M., Ponette, Q., 2008. Influence of species and rain event characteristics on stemflow volume in a temperate mixed oak-beech stand. Hydrol. Process. 22, 4455–4466.

Aussenac, G., 1970. Action du couvert forestier sur la distribution au sol des précipitations. Annales des Sciences Forestières 27, 383–399.

Bellot, J., Àvila, A., Rodrigo, A., 1999. Throughfall Stemflow 137, 209–222.

Bolte, A., Ammer, C., Löf, M., Madsen, P., Nabuurs, G.-J., Schall, P., Spathelf, P., Rock, J., 2009. Adaptive forest management in central Europe: climate change impacts, strategies and integrative concept. Scand. J. For. Res. 24, 473–482.

Bolte, A., Czajkowski, T., Kompa, T., 2007. The north-eastern distribution range of European beech a review. Forestry 80, 413–429.

Bouten, W., Heimovaara, T.J., Tiktak, A., 1992. Spatial patterns of throughfall and soil water dynamics in a Douglas fir stand. Water Resour. Res. 28, 3227–3233.

Bréda, N., Granier, A., Barataud, F., Moyne, C., 1995. Soil water dynamics in an oak stand. Plant Soil 172, 17–27.

Bréda, N., Huc, R., Granier, A., Dreyer, E., 2006. Temperate forest trees and stands under severe drought: a review of ecophysiological responses, adaptation processes and long-term consequences. Ann. Forest Sci. 63, 625–644.

Canadell, J., Jackson, R.B., Ehleringer, J.B., Mooney, H.A., Sala, O.E., Schulze, E.D., 1996. Maximum rooting depth of vegetation types at the global scale. Oecologia 108, 583–595.
Cheaib, A., Badeau, V., Boe, J., Chuine, I., Delire, C., Dufrene, E., Francois, C., Gritti, E.S., Legay, M., Page, C., Thuiller, W., Viovy, N., Leadley, P., 2012. Climate change impacts on tree ranges: model intercomparison facilitates understanding and quantification of uncertainty. Ecol. Lett. 15, 533–544.
Ciais, P., Reichstein, M., Viovy, N., Granier, A., Ogee, J., Allard, V., Aubinet, M., Buchmann, N., Bernhofer, C., Carrara, A., Chevallier, F., De Noblet, N., Friend, A. D., Friedlingstein, P., Grunwald, T., Heinesch, B., Keronen, P., Knohl, A., Krinner, G., Loustau, D., Manca, G., Matteucci, G., Miglietta, F., Ourcival, J.M., Papale, D., Pilegaard, K., Rambal, S., Seufert, G., Soussana, J.F., Sanz, M.J., Schulze, E.D., Vesala, T., Valentini, R., 2005. Europe-wide reduction in primary productivity caused by the heat and drought in 2003. Nature 437, 529–533.
Decourt, N., 1973. Production primaire, production utile: méthodes d'évaluation, indices de productivité. Annales des Sciences Forestières 30, 219–237.
Estrada-Medina, H., Graham, R.C., Allen, M.F., Jiménez-Osornio, J.J., Robles-Casolco, S., 2012. The importance of limestone bedrock and dissolution karst features on tree root distribution in northern Yucatán, México. Plant Soil 362, 37–50.
Fang, J., Lechowicz, M.J., 2006. Climatic limits for the present distribution of beech (*Fagus* L.) species in the world. J. Biogeogr. 33, 1804–1819.
FAO, 2016. World reference base for soil resources 2014. In: World Soil Resources Report 106. FAO, Rome.
Fernández-Martínez, M., Vicca, S., Janssens, I.A., Sardans, J., Luyssaert, S., Campioli, M., Chapin Iii, F.S., Ciais, P., Malhi, Y., Obersteiner, M., Papale, D., Piao, S.L., Reichstein, M., Rodà, F., Peñuelas, J., 2014. Nutrient availability as the key regulator of global forest carbon balance. Nat. Climate Change 4, 471–476.
Fransen, B., de Kroon, H., Berendse, F., 1998. Root morphological plasticity and nutrient acquisition of perennial grass species from habitats of different nutrient availability. Oecologia 115, 351–358.
Gale, M.R., Grigal, D.F., 1987. Vertical root distributions of northern tree species in relation to successional status. Can. J. For. Res. 17, 829–834.
Genet, A., Wernsdörfer, H., Jonard, M., Pretzsch, H., Rauch, M., Ponette, Q., Nys, C., Legout, A., Ranger, J., Vallet, P., Saint-André, L., 2011. Ontogeny partly explains the apparent heterogeneity of published biomass equations for Fagus sylvatica in central Europe. For. Ecol. Manage. 261, 1188–1202.
Geßler, A., Keitel, C., Kreuzwieser, J., Matyssek, R., Seiler, W., Rennenberg, H., 2006. Potential risks for European beech (*Fagus sylvatica* L.) in a changing climate. Trees 21, 1–11.
Goisser, M., Zang, U., Matzner, E., Borken, W., Häberle, K.-H., Matyssek, R., 2013. Growth of juvenile beech (*Fagus sylvatica* L.) upon transplant into a wind-opened spruce stand of heterogeneous light and water conditions. For. Ecol. Manage. 310, 110–119.
Göransson, H., Ingerslev, M., Wallander, H., 2008. The vertical distribution of N and K uptake in relation to root distribution and root uptake capacity in mature Quercus robur, Fagus sylvatica and Picea abies stands. Plant Soil 306, 129–137.
Granier, A., Biron, P., Lemoine, D., 2000a. Water balance, transpiration and canopy conductance in two beech stands. Agric. For. Meteorol. 100, 291–308.
Granier, A., Bréda, N., Biron, P., Villette, S., 1999. A lumped water balance model to evaluate duration and intensity of drought constraints in forest stands. Ecol. Model. 116, 269–283.
Granier, A., Loustau, D., Bréda, N., 2000b. A generic model of forest canopy conductance dependent on climate, soil water availability and leaf area index. Ann. Forest Sci. 57, 755–765.
Granier, A., Reichstein, M., Bréda, N., Janssens, I.A., Falge, E., Ciais, P., Grünwald, T., Aubinet, M., Berbigier, P., Bernhofer, C., Buchmann, N., Facini, O., Grassi, G., Heinesch, B., Ilvesniemi, H., Keronen, P., Knohl, A., Köstner, B., Lagergren, F., Lindroth, A., Longdoz, B., Loustau, D., Mateus, J., Montagnani, L., Nys, C., Moors, E., Papale, D., Peiffer, M., Pilegaard, K., Pita, G., Pumpanen, J., Rambal, S., Rebmann, C., Rodrigues, A., Seufert, G., Tenhunen, J., Vesala, T., Wang, Q., 2007. Evidence for soil water control on carbon and water dynamics in European forests during the extremely dry year: 2003. Agric. For. Meteorol. 143, 123–145.
Henry, M., Picard, N., Trotta, C., Manlay, R., Valentini, R., Bernoux, M., Saint-André, L., 2011. Estimating tree biomass of sub-Saharan African forests: a review of available allometric equations. Silva Fennica 45.
Hentschel, R., Hommel, R., Poschenrieder, W., Grote, R., Holst, J., Biernath, C., Gessler, A., Priesack, E., 2015. Stomatal conductance and intrinsic water use efficiency in the drought year 2003: a case study of European beech. Trees 30, 153–174.
Hlásny, T., Mátyás, C., Seidl, R., Kulla, L., Merganičová, K., Trombik, J., Dobor, L., Barcza, Z., Konôpka, B., 2014. Climate change increases the drought risk in Central European forests: what are the options for adaptation? Forest. J. 60.
Huang, M., Zettl, J.D., Barbour, S.L., Elshorbagy, A., Si, B.C., 2013. The impact of soil moisture availability on forest growth indices for variably layered coarse-textured soils. Ecohydrology 6, 214–227.
IPCC, 2014. Climate change 2014: impacts, adaptation, and vulnerability. Part A: Global and sectoral aspects. In: Field, C.B., Barros, V.R., Dokken, D.J., Mach, K.J., Mastrandrea, M.D., Bilir, T.E., Chatterjee, M., Ebi, K.L., Estrada, Y.O., Genova, R.C., Girma, B., Kissel, E.S., Levy, A.N., MacCracken, S., Mastrandrea, P.R., White, L.L. (Eds.), Contribution of Working Group II to the Fifth Assessment Report of the Intergovernmental Panel on Climate Change. Cambridge University Press, Cambridge, United Kingdom and New York, NY, USA.
Jackson, R.B., Manwaring, J.H., Caldwell, M.M., 1990. Rapid physiological adjustment of roots to localized soil enrichment. Nature 344, 58–60.
Jackson, R.B., Moore, L.A., Hoffmann, W.A., Pockman, W.T., Linder, C.R., 1999. Ecosystem rooting depth determined with caves and DNA. Proc. Natl. Acad. Sci. 96, 11387–11392.
Jamagne, M., 2011. Grands paysages pédologiques de France.
Knutzen, F., Meier, I.C., Leuschner, C., 2015. Does reduced precipitation trigger physiological and morphological drought adaptations in European beech (*Fagus sylvatica* L.)? Comparing provenances across a precipitation gradient. Tree Physiol. 35, 949–963.
Köcher, P., Gebauer, T., Horna, V., Leuschner, C., 2009. Leaf water status and stem xylem flux in relation to soil drought in five temperate broad-leaved tree species with contrasting water use strategies. Ann. Forest Sci. 66. 101-101.
Kramer, K., Degen, B., Buschbom, J., Hickler, T., Thuiller, W., Sykes, M.T., de Winter, W., 2010. Modelling exploration of the future of European beech (*Fagus sylvatica* L.) under climate change—range, abundance, genetic diversity and adaptive response. For. Ecol. Manage. 259, 2213–2222.
Lebourgeois, Differt, Granier, Breda, Ulrich, 2006. Premières observations phénologiques des peuplements du réseau national de suivi à long terme des écosystèmes forestiers (Renecofor). Revue Forestière Française 407.
Lebourgeois, F., Bréda, N., Ulrich, E., Granier, A., 2005. Climate-tree-growth relationships of European beech (*Fagus sylvatica* L.) in the French Permanent Plot Network (RENECOFOR). Trees 19, 385–401.
Lewis, D.C., Burgy, R.H., 1964. The relationship between oak tree roots and groundwater in fractured rock as determined by tritium tracing. J. Geophys. Res. 69, 2579–2588.
Lindner, M., Maroschek, M., Netherer, S., Kremer, A., Barbati, A., Garcia-Gonzalo, J., Seidl, R., Delzon, S., Corona, P., Kolström, M., Lexer, M.J., Marchetti, M., 2010. Climate change impacts, adaptive capacity, and vulnerability of European forest ecosystems. For. Ecol. Manage. 259, 698–709.
Medlyn, B.E., Duursma, R.A., Zeppel, M.J.B., 2011. Forest productivity under climate change: a checklist for evaluating model studies. Wiley Interdisciplinary Rev.: Climate Change 2, 332–355.
Meehl, G.A., Tebaldi, C., 2004. More intense, more frequent, and longer lasting heat waves in the 21st century. Science 305, 994–997.
Moore, G.W., Bond, B.J., Jones, J.A., 2011. A comparison of annual transpiration and productivity in monoculture and mixed-species Douglas-fir and red alder stands. For. Ecol. Manage. 262, 2263–2270.
Mun, H.T., 1988. Comparisons of primary production and nutrients absorption by aMiscanthus sinensis community in different soils. Plant Soil 112, 143–149.
Neilson, R.P., King, G.A., Koerper, G., 1992. Toward a rule-based biome model. Landscape Ecol. 7, 27–43.
Oishi, A.C., Oren, R., Novick, K.A., Palmroth, S., Katul, G.G., 2010. Interannual invariability of forest evapotranspiration and its consequence to water flow downstream. Ecosystems 13, 421–436.
Oren, R., Ewers, B.E., Todd, P., Phillips, N., Katul, G., 1998. Water balance delineates the soil layer in which moisture affects canopy conductance. Ecol. Appl. 8, 990–1002.
Penman, H.L., 1948. Natural evaporation from open water, bare soil and grass. Proc. Roy. Soc. A: Math., Phys. Eng. Sci. 193, 120–145.
Picard, N., Henry, M., Mortier, F., Trotta, C., Saint-André, L., 2012. Using bayesian model averaging to predict tree aboveground biomass in tropical moist forests. Forest Sci. 58, 15–23.
Piedallu, C., Gégout, J.-C., Bruand, A., Seynave, I., 2011. Mapping soil water holding capacity over large areas to predict potential production of forest stands. Geoderma 160, 355–366.
Power, S.A., 1994. Temporal trends in twig growth of *Fagus sylvatica* L. and their relationships with environmental factors. Forestry 67, 13–30.
Robinson, D., 1996. Resource capture by localized root proliferation: why do plants bother? Ann. Bot. 77, 179–186.
Rosling, A., Landeweert, R., Lindahl, B.D., Larsson, K.H., Kuyper, T.W., Taylor, A.F.S., Finlay, R.D., 2003. Vertical distribution of ectomycorrhizal fungal taxa in a podzol soil profile. New Phytol. 159, 775–783.
Rowell, D.P., Jones, R.G., 2006. Causes and uncertainty of future summer drying over Europe. Clim. Dyn. 27, 281–299.
Saint-André, L., M'Bou, A.T., Mabiala, A., Mouvondy, W., Jourdan, C., Roupsard, O., Deleporte, P., Hamel, O., Nouvellon, Y., 2005. Age-related equations for above- and below-ground biomass of a Eucalyptus hybrid in Congo. For. Ecol. Manage. 205, 199–214.
Sala, O.E., Parton, W.J., Joyce, L.A., Lauenroth, W.K., 1988. Primary production of the central grassland region of the United States. Ecology 69, 40–45.
Sampson, D.A., Allen, H.L., 1999. Regional influences of soil available water-holding capacity and climate, and leaf area index on simulated loblolly pine productivity. For. Ecol. Manage. 124, 1–12.
Schar, C., Vidale, P.L., Luthi, D., Frei, C., Haberli, C., Liniger, M.A., Appenzeller, C., 2004. The role of increasing temperature variability in European summer heatwaves. Nature 427, 332–336.
Schipka, F., Heimann, J., Leuschner, C., 2005. Regional variation in canopy transpiration of Central European beech forests. Oecologia 143, 260–270.
Schwärzel, K., Feger, K.-H., Häntzschel, J., Menzer, A., Spank, U., Clausnitzer, F., Köstner, B., Bernhofer, C., 2009a. A novel approach in model-based mapping of soil water conditions at forest sites. For. Ecol. Manage. 258, 2163–2174.
Schwärzel, K., Menzer, A., Clausnitzer, F., Spank, U., Häntzschel, J., Grünwald, T., Köstner, B., Bernhofer, C., Feger, K.-H., 2009b. Soil water content measurements deliver reliable estimates of water fluxes: a comparative study in a beech and a spruce stand in the Tharandt forest (Saxony, Germany). Agric. For. Meteorol. 149, 1994–2006.

Seynave, I., Gégout, J.-C., Hervé, J.-C., Dhôte, J.-F., 2008. Is the spatial distribution of European beech (*Fagus sylvatica* L.) limited by its potential height growth? J. Biogeogr. 35, 1851–1862.

Tarp, P., Helles, F., Holten-Andersen, P., Bo Larsen, J., Strange, N., 2000. Modelling near-natural silvicultural regimes for beech – an economic sensitivity analysis. For. Ecol. Manage. 130, 187–198.

Tetegan, M., Nicoullaud, B., Baize, D., Bouthier, A., Cousin, I., 2011. The contribution of rock fragments to the available water content of stony soils: proposition of new pedotransfer functions. Geoderma 165, 40–49.

Turpault, M.-P., Nys, C., Calvaruso, C., 2009. Rhizosphere impact on the dissolution of test minerals in a forest ecosystem. Geoderma 153, 147–154.

Zwieniecki, M.A., Newton, M., 1995. Roots growing in rock fissures: their morphological adaptation. Plant Soil 172, 181–187.